Numerical Analysis of Punching Shear Failure Mechanism and Strength of Open Sandwich Slab

Ahmed Farghaly*, Tamon Ueda**, and Hitoshi Furuuchi***

* M. of Eng., Div. of Str. & Geotech. Eng., Hokkaido University, Kita-ku, Sapporo 060-8628
** Dr. of Eng., Div. of Str. & Geotech. Eng., Hokkaido University, Kita-ku, Sapporo 060-8628
***B. of Eng., Div. of Str. & Geotech. Eng., Hokkaido University, Kita-ku, Sapporo 060-8628

Effort has been given using non-linear 3D FEM program to predict the punching shear failure mechanism and its strength of steel-concrete open sandwich slabs with stud. In the analysis the stud is modeled by link element whose constitutive model is derived from the authors' experimental study. The results show very good agreement between the analytical and experimental values. Punching shear failure phenomena is carefully examined in the analysis observing predicted concrete cracking pattern and concrete crushing. Based on the analytical observation a quantitative study on factors, such as concrete strength and plate thickness, has been done to develop an analytical expression to compute the punching shear strength of open sandwich slab.
Key Words: FEM analysis, open sandwich slab, punching shear failure

1. Introduction

The problem of the punching shear strength of reinforced concrete slabs subjected to concentrated loads has received great attention over several decades because of its importance in many of structure systems such as flat slab or bridge deck. The ultimate strength of such slabs is often determined by the punching shear failure load, which is generally smaller than the flexural failure load calculated by theories such as yield line theory. Many variables have a marked effect on the punching shear strength of slabs. Most research on the punching shear strength of slabs has been concerned with the generation of experimental data on simply supported slabs and the development of empirical equation.

A few theoretical analyses have also been proposed by various investigators based on different models. The lack of a simple theoretical model to compute the punching shear strength is due to the complexities of the basic three-dimensional behavior of the slab.

Constant need for cost-effective structural forms has led to the increasing use of composite construction. Significant economy has been observed in this form of construction. Composite steel-concrete structures are used widely in modern bridge and building construction.

A composite member is formed when a steel component, such as an I-section beam, is attached to a concrete component, such as a floor slab or bridge deck. In such a composite T-beam the comparatively high strength of the concrete in compression complements the high strength of the steel in tension. In the composite T-beam the steel top flange, which the studs have been attached to, has no deformation (local bending) because the web prevents the deformation from taking place in the flanges. Meanwhile, in the case of open sandwich slab the steel plate may be affected by the local bending at the position of the studs because there is no web underneath. However, the local bending can not be considered in this study because the stud is modeled by a spring element. Only a few numbers of studies have so far been made on mechanism of punching shear failure of open sandwich slab. Besides, there is no reasonable method for the prediction of the punching shear failure load with acceptable accuracy.

Three-dimensional behavior is common to both RC and sandwich slabs. Thus, there is the same difficulty in modeling open sandwich slabs. Moreover, for the open sandwich slab the difficulty is due to the uncertain shear transfer mechanism that exists in the slab before failure.

The purpose of this paper is to present a simple analytical model for the punching shear strength of open sandwich slab. It is based on results obtained using 3D FEM program as a numerical simulation tool of the failure mechanism. The 3D FEM analysis is shown to be efficient in simulating punching shear failure for which a sensitivity analysis has been performed. Consequently and opposed to most of the existing analytical models, the proposed model is not based on empirical coefficient because parameters are derived from numerical simulations of different slabs. It is shown that the analysis presented can develop a good theoretical model to predict the punching shear strength of open sandwich slabs.

Table 1 - Material Properties and Details of Specimens

	E_c (GPa)	f'_c (MPa)	f_t (MPa)	μ_c	E_s (GPa)	f_y (MPa)	μ_s	d (mm)	a (mm)	a/d	h_s (mm)	s (mm)	t_s (mm)
A1	27.7	31.0	2.30	0.20	200	281	0.30	150	250	1.7	80	140	6
A2	27.7	31.0	2.30						550	3.7			
A3	21.0	15.0	1.40						400	2.7			
T3	26.4	27.6	2.12										
A5	33.5	52.0	3.20										
S1	26.0	26.5	2.06		170	300		175	450	2.6	50	100	16
S2	26.0	26.4	2.06		175	284							9
S3	22.7	18.5	1.60		170	284							4.5

where

E_c	Modulus of elasticity of concrete
E_s	Modulus of elasticity of steel
f'_c	Concrete compressive strength
f_t	Concrete tensile strength
f_y	Steel yielding strength
d	Depth of slab
a/d	Shear span depth ratio
h_s	Height of stud
s	Spacing between studs
t_s	Thickness of steel plate

2. Description of Experimented Slabs

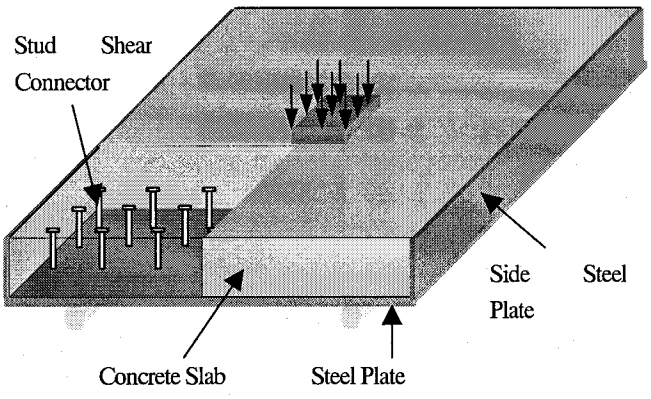

Fig. 1 Open Sandwich Slab

Eight open sandwich slabs were cast and tested. The parameters of the experimental program were; concrete compressive strength, shear span to depth ratio, and thickness of steel plate. As listed in Table 1.

Stud shear connectors were provided at the interface between concrete and steel plate. The shear connectors were welded perpendicular to the steel plate. The load was given to a square loading plate (10x10 cm). The specimens were designed to fail due to punching shear failure (see Fig. 1).

3. Out line of Analysis

3.1 Finite Element Program

The three-dimensional computational simulation tool developed in Hokkaido University [1] was revised by the authors to analyze punching shear failure of steel-concrete open sandwich members. It is based on the finite element method and reproduces the nonlinear material behavior characterizing composite structures by superimposing the elasto-plastic behavior of steel plate and the tensile crack of the concrete. For non-linear computation, Newton-Raphson method was applied. Iteration was continued until the convergence for residual displacement caused by unbalanced force was satisfied. For constitutive law of concrete before cracking, three-dimensional elasto-plastic and fracture model [2] was applied which consider the effect of the confinement, deformability and the bi-axial compression in the concrete constitutive law. A three-dimensional failure criteria in tension-tension and tension-compression was developed by modifying an existing two-dimensional failure criteria. Also, constitutive model for concrete after cracking has been applied [3]. When the first crack occurs, the strains in global coordinate system are transformed into the strains in local coordinate system (called as crack coordinate system). In case of the second crack, one of two axes in the plane is coincided with direction of the intersecting line between first and second crack plane. Two local systems share one of their axes and another axes in the plane is in the direction where the crack opens. After calculating stresses from the strains in the crack coordinate system by some constitutive laws, the stresses are retransformed into stresses in the global coordinate system and averaged. Furthermore, solution of bond link problems for steel-concrete composite slab was developed. The proposed model that adopts the transferred shear force-relative displacement relationship for stud shear connector was used in this study [4].

3.2 Analytical Method

Analysis of punching shear failure of open sandwich slab was

conducted to study the mechanism of failure. Eleven analytical specimens for open sandwich slab, where bond link element was adopted for stud between concrete and steel, were modeled.

Figs. 2 and 3 show the finite element mesh. Because of symmetry, a quarter of the open sandwich slabs was analyzed. Prescribed displacements were given at the loading point directly which is a steel element connected directly to the concrete element. The material properties and details of specimens used for the analysis are shown in Table 1. The tensile strength and modulus of elasticity of concrete were calculated from the compressive strength and Poisson's ratio was 0.2 [5]. All other properties were measured at experiment. Discrete way of representation by the bond link element was used. On beam test, the strain distribution of the steel plate had been calculated around the studs. High strain has been observed in the area of 4x4 cm around the studs. Therefore, the effective area for stud has been decided as 16 cm^2 (4x4 cm) [4].

Moreover, the smeared way also has been used for one specimen to confirm the effect of the way of meshing whether discrete or smeared on the analytical result of the slabs. Fig. 3(d) shows the finite element mesh for slab A3 by the smeared way meshing.

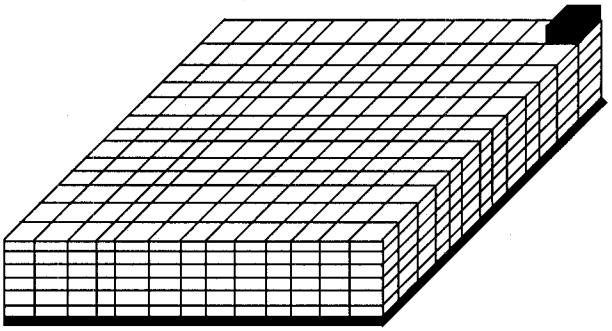

Fig. 2 Illustration of Finite Element Mesh

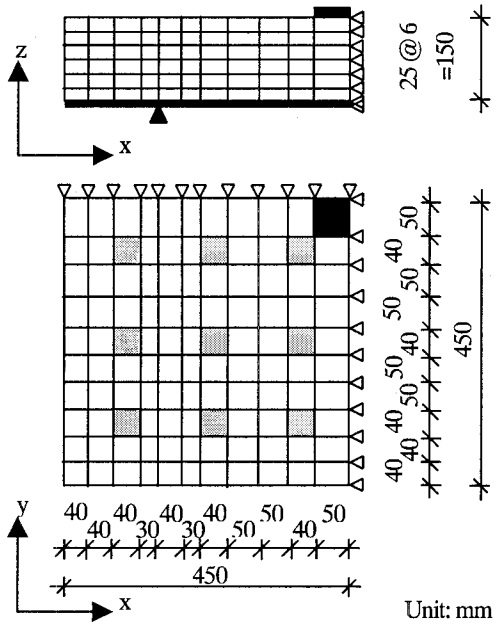

Fig. 3(a) Finite Element Mesh of slab A1

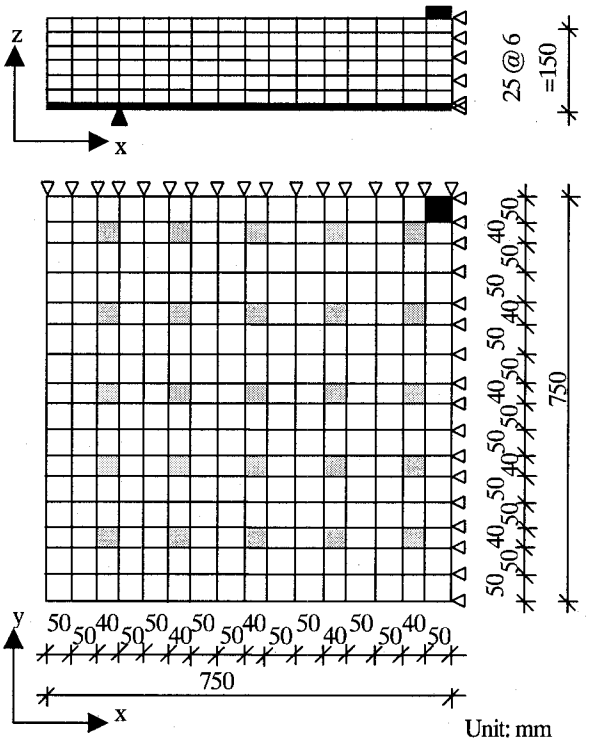

Fig. 3(b) Finite Element Mesh of slab A2

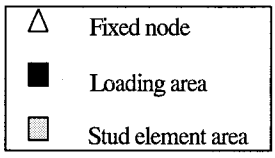

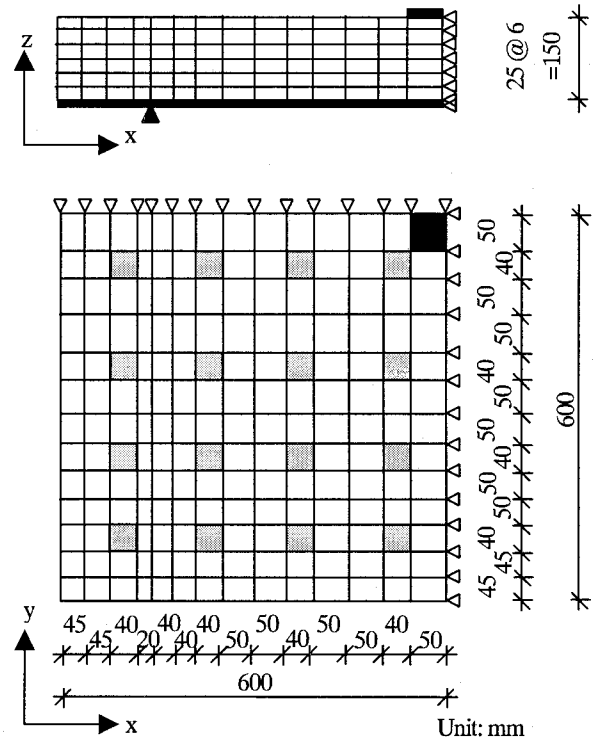

Fig. 3(c) Finite Element Mesh of A3, T3 and A5 (Discrete way)

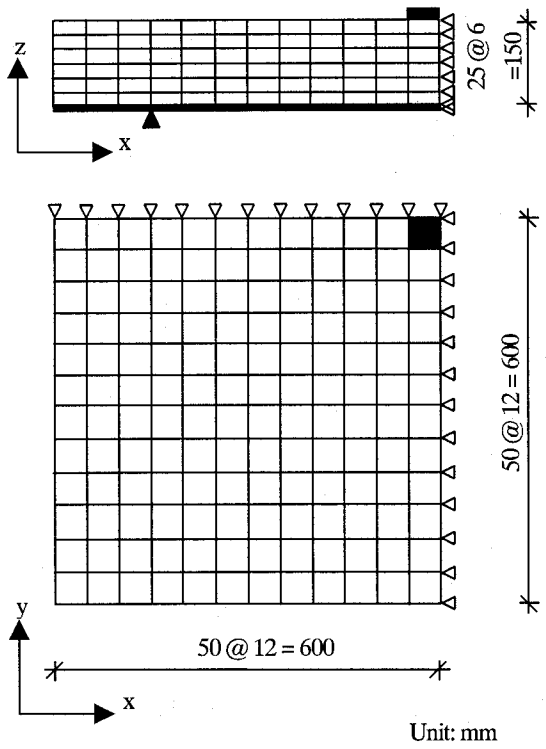

Fig. 3(d) Finite Element Mesh of A3
(Smeared way)

Fig. 3 Finite Element Mesh of Analytical Specimens

4. Results and Discussion

4.1 Comparison of Experimental and Analytical Results

(1) Ultimate Load

The ultimate load, in experiment, was reached due to punching shear failure in all specimens except for slab A1 that failed due to anchorage failure. The FEM calculation was stopped after the peak load was observed. The ultimate loads are shown in Table 2. It is clearly seen that the predicted loads agree with the experimental ones. Comparison of the ultimate load of specimens A1 and A2, which have the same concrete compressive strength, shows that it increases with the increase of the shear span to depth ratio. It is believed that punching shear strength decreases as shear span to depth ratio increases but the number of studs were too small to develop fully punching shear strength in specimen A1.

Therefore the punching shear strength of specimen A1 was less than the punching shear strength of A2. Moreover, the comparison of the other specimens, which have study the concrete compressive strength and thickness of steel plates effects, shows that the punching shear capacity increases with the increase of the value of the parameter.

Table 2. Ultimate Loads

Specimen	Exp. (KN)	Ana. (KN)	$\frac{\text{Exp.}}{\text{Ana.}}$
A1	388.8	417.0	0.93
A2	494.0	477.1	1.03
A3	225.0	249.2	0.90
T3	398.8	395.4	1.01
A5	566.9	564.2	1.00
S1	440.8	459.2	0.96
S2	414.3	438.5	0.94
S3	291.3	301.1	0.97

(2) Deflection

Experimental and predicted relationships between applied load and deflection of the analyzed slab specimens are shown in Fig. 4. It can be said that the analysis can estimate the experimental behavior reasonably. By comparing the analytical results with the experimental ones, we can find that the Load-Deflection curves for analysis have the same behavior as the experimental curves for all specimens except for slab A1 that could be probably due to experimental scatter. Therefore, in the elastic stage of slab A1, we can notice the agreement between the analytical and the experimental results, but when the cracks started to propagate the anchorage failure occurred and caused a reduction of the stiffness. Meanwhile, the predicted ultimate load agrees with the experimental one.

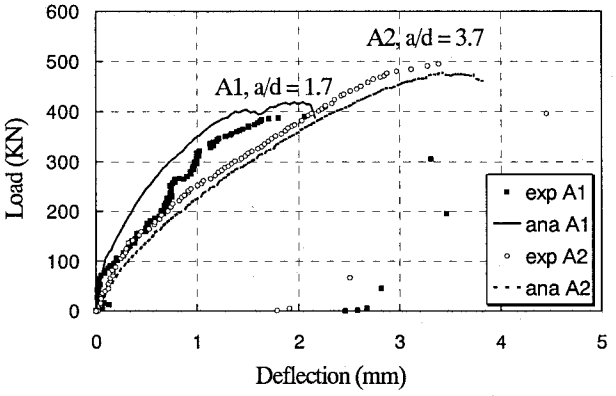

Fig. 4(a) Load-Deflection of slabs A1 and A2

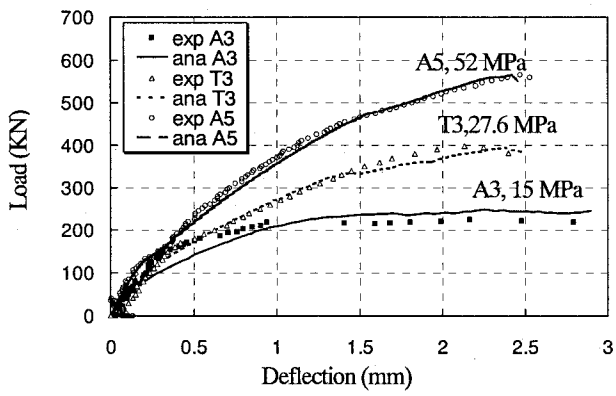

Fig. 4(b) Load-Deflection of slabs A3, T3, and A5

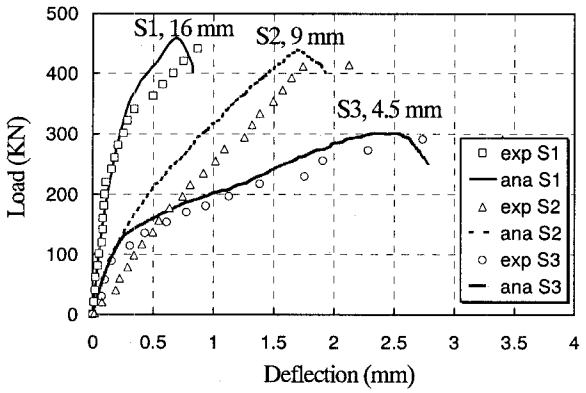

Fig. 4(c) Load-Deflection of slabs S1, S2, and S3

(3) Discrete and Smeared Meshing

In the case of discrete meshing stiffness of each stud is only allocated in the stud link element (see the elements in gray color), the effective area of the stud. In the case of smeared meshing, however, the stiffness of studs has spread all over the plane area of the slab.

For the comparison between the discrete and the smeared way of analysis, Fig. 4(d) shows the analytical curves for slab A3 analyzed by the two ways of meshing. From the figure we can notice that, the way of meshing has no effect on the initial stiffness until it reaches plastic region where the behavior starts to change. Also, it was found that the ultimate load obtained by the discrete meshing is closer to the experimental result than the smeared meshing. Therefore, discrete way of meshing is considered to be the appropriate way to analyze the open sandwich slabs and has been used through out this study.

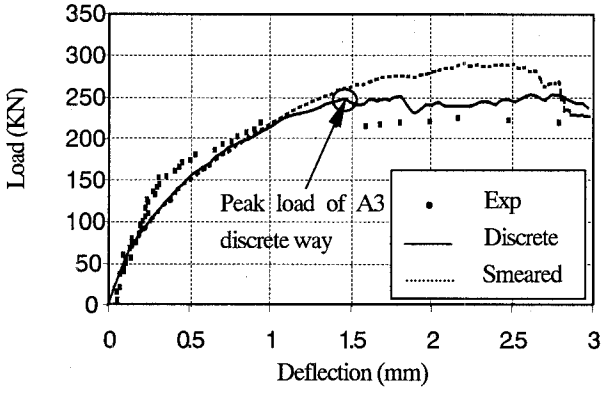

Fig. 4(d) Comparison between Discrete and Smeared Way of Analysis of Slab A3

4.2 Strain Distribution

Fig. 5 shows strain distribution along height under loading plate of the analyzed specimens. There is little difference when the applied load is about 10% of peak load, as no crack occurred at that load level, however, when the applied load is at 90% of the peak load it is clear that the depth of the neutral axis of slab A1 is almost same as of slab A2 which indicates that the shear span to depth ratio has no effect on the position of the neutral axis. Meanwhile, in case of different concrete compressive strength shows the effect on the position of the neutral axis as the comparison between slabs A3, T3 and A5 shows. Moreover, it was found that the thickness of the steel plate has a clear effect on the position of the neutral axis that the depth of the neutral axis is increasing with the decreasing the thickness of steel plate. Though the position of neutral axis could be one of the indicator, there are many mechanisms involved that have a sizeable effect on punching shear capacity of slab. They are mutually related to each other, which make the total procedure more complex.

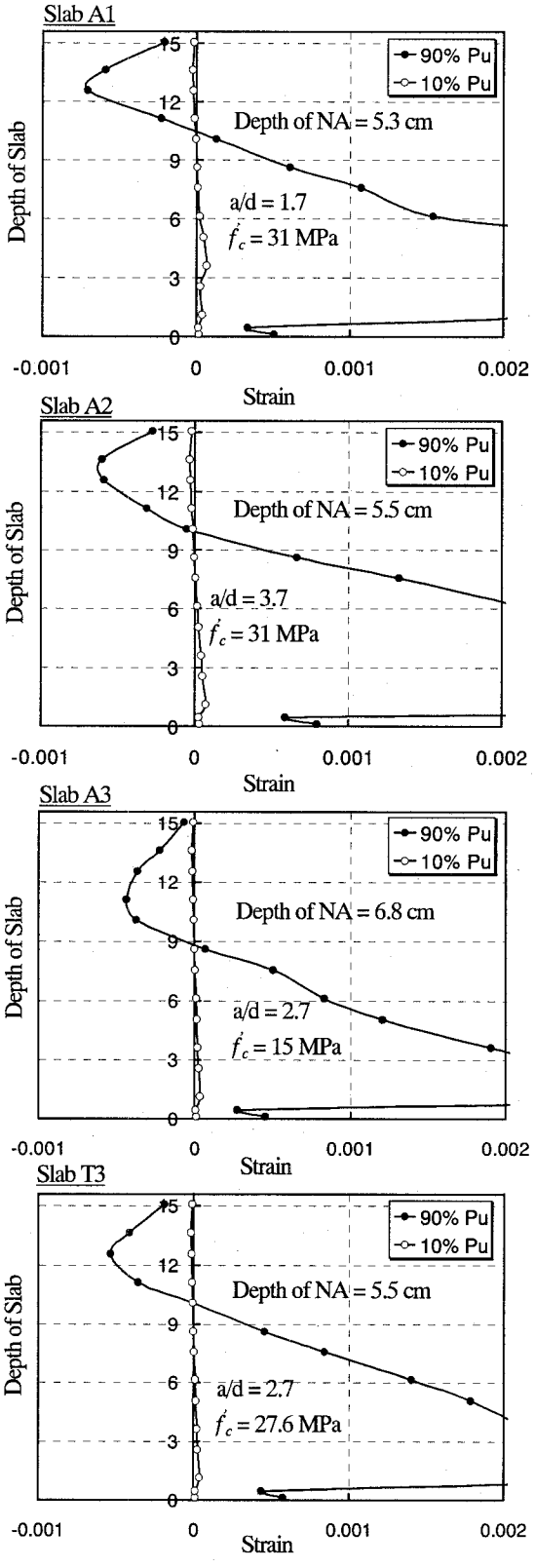

Fig. 5 Strain Distribution

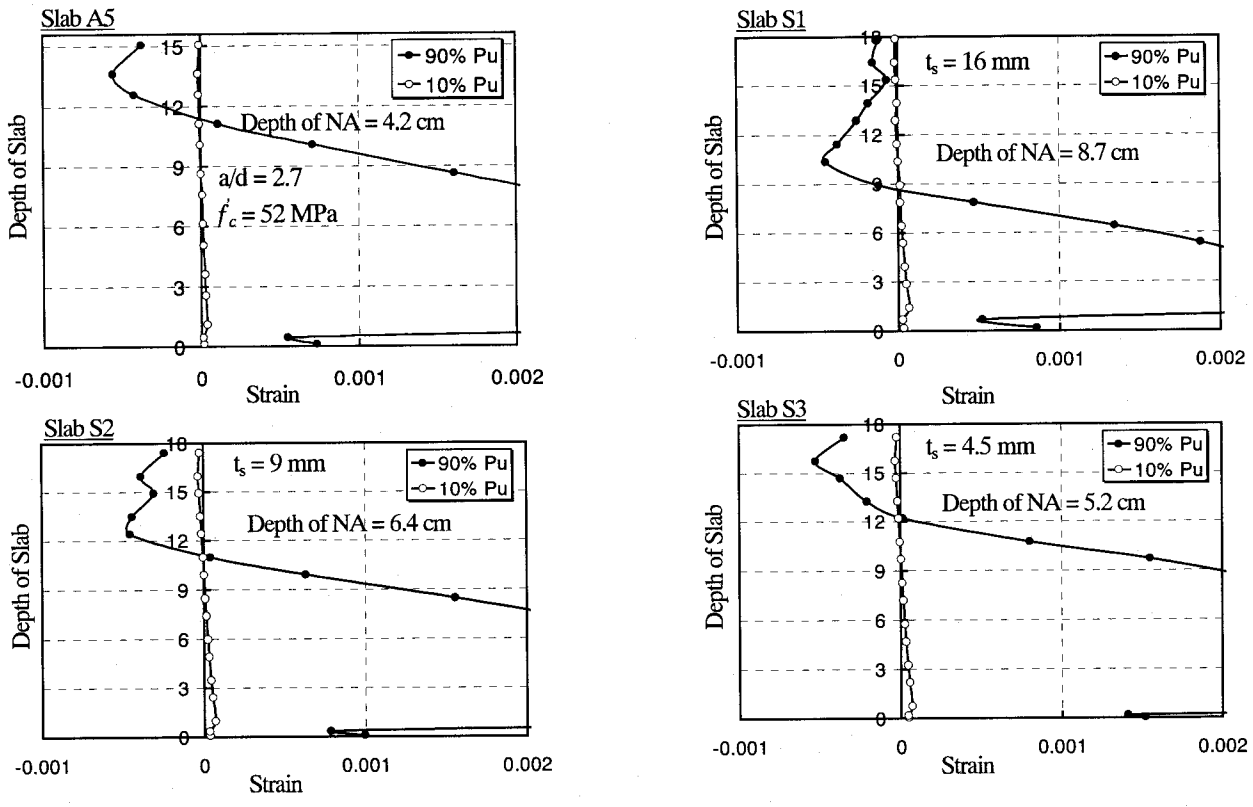

Fig. 5 Strain Distribution (continue)

5. Open Sandwich Slab Failure Mechanism

5.1 Preliminaries

Fig. 6 shows illustration of the crack formation, Fig. 7 illustrates the layers position, and Fig. 8 shows the crack pattern at the peak load, the marks express the cracks' direction at the gauss points.

Application of an increasing load to a slab that is monolithically connected to the load cell implies the sequence of a number of events such as (see Fig. 6);

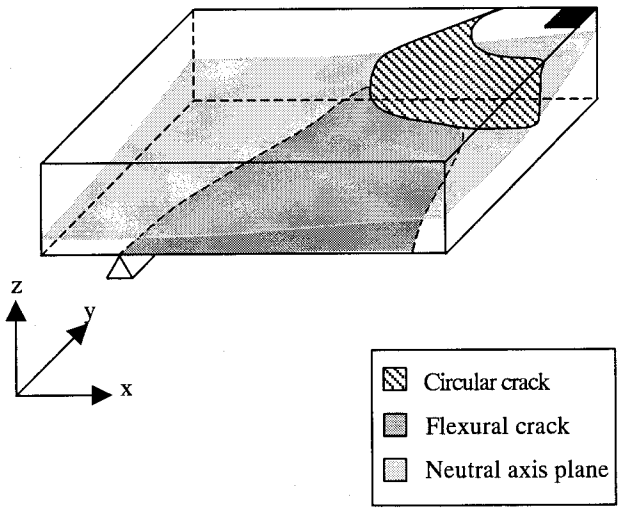

Fig. 6 Illustration of the Crack Formation

(1) The formation of a roughly circular crack around the loading area from the top layers of the concrete on the compression surface and its subsequent propagation up to almost the plane of neutral axis of the slab (layers 1, 2, and 3 in Figs. 7 and 8).

(2) On the mean time, formation of new diagonal flexural cracks in the lower concrete layers, which started to propagate from the plane of neutral axis (layer 4) toward the end side of the slab until they spread in all concrete elements near the bottom surface (layer 8). Moreover, the crack pattern of layer 8 (which is the nearest layer to the steel plate) shows that the crack has been propagated and localized at the positions of the studs, which simulates the real behavior of the open sandwich slabs.

(3) The initiation of the diagonal flexural crack observed at about 50-70 % of the ultimate load.

(4) With increasing loads the inclined circular crack develops towards the compression zone, but at the final stage, its propagation is prevented by the compression zone above the top of the crack near the loading plate as there were no cracks occurred on the concrete element under the loading plate (layers 1, 2, and 3 in Figs. 7 and 8).

(5) Finally, punching shear failure occurs in the compression zone due to crushing of the concrete near to the loading plate. This phenomenon agrees with the experimental result Moreover, it was found that, the concrete layers near the top surface (or compression edge) crushed earlier than the concrete layer far from the top surface, in other word, the concrete at layer 1 crushed at 80% of the peak load meanwhile, the concrete at layer 4 crushed at 97% of the peak load.

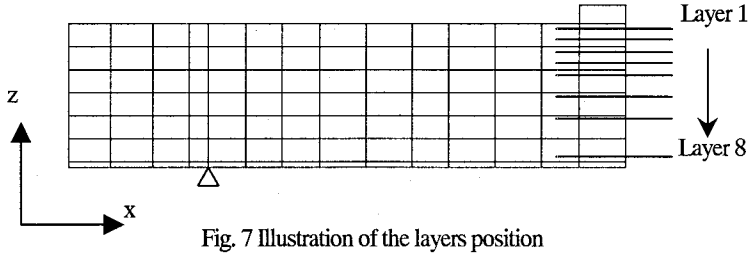

Fig. 7 Illustration of the layers position

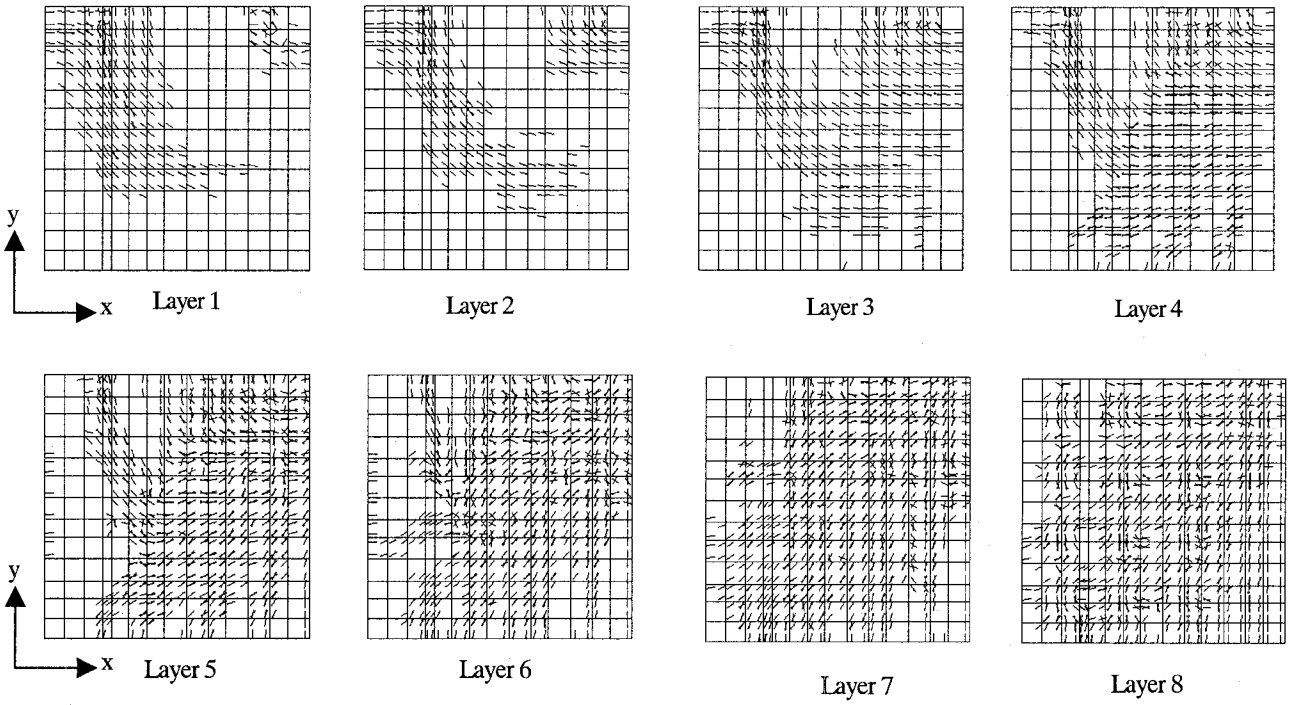

Fig. 8 Crack Pattern at Peak Load of Slab A3

5.2 Effect of Concrete Compressive Strength

Comparison between the three slabs A3, T3 and A5 implies that the radius of the circular cracks around the loading area is increasing as the concrete compressive strength decreases.

Moreover, the diagonal flexural cracks started to propagate in the case of less concrete compressive strength before its propagation in case of higher concrete compressive strength.

Furthermore, the investigation shows that the inclination of the principal stresses under the loading point is almost zero degree. This inclination increases as the distance from the loading point increases until it reaches the maximum value near the support (see Fig. 9). Also, the principal stresses were found to increase as the distance from the loading point decreases.

Fig. 10 shows the neutral axis lines for different concrete compressive strength. It is observed that the depth of the neutral axis increases as the modulus of elasticity increases. However, as a matter of fact, the modulus of elasticity is proportional to the concrete compressive strength.

Therefore, the depth of the neutral axis and the concrete copressive strength can be related to each other in indirect way. Thus, it can be said that, the depth of the neutral axis increases as the concrete compressive strength increases (reduction of the compression zone).

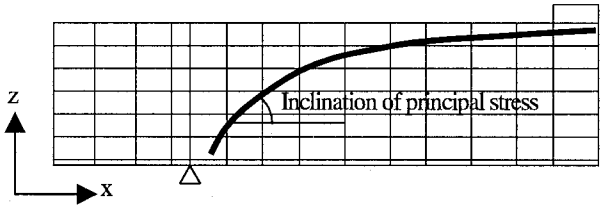

Fig. 9 Inclination of Principle Stresses along shear span

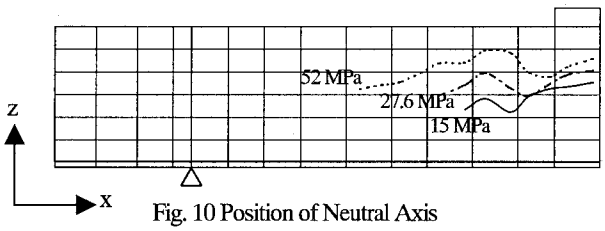

Fig. 10 Position of Neutral Axis

Fig. 11 shows crack pattern in a section elevation view of the analytical slabs at the peak load at the mid span of the slabs. It is clearly seen that the cracking angle has not changed as the concrete compressive strength changed.

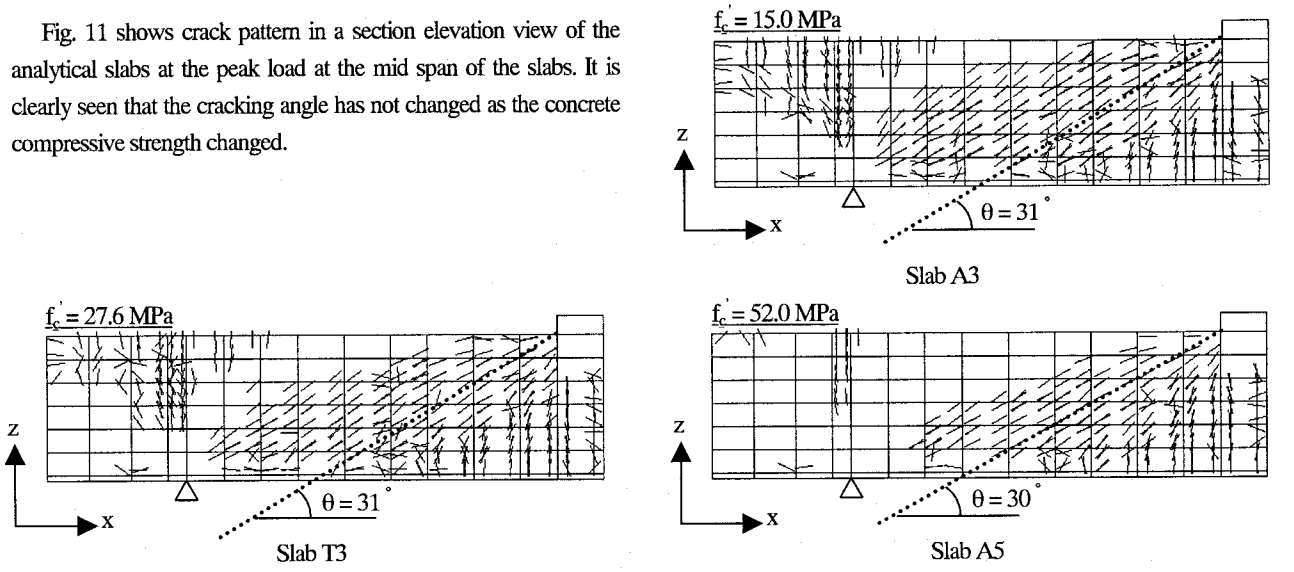

Fig. 11 Crack Pattern of Analytical Slabs at Peak Load

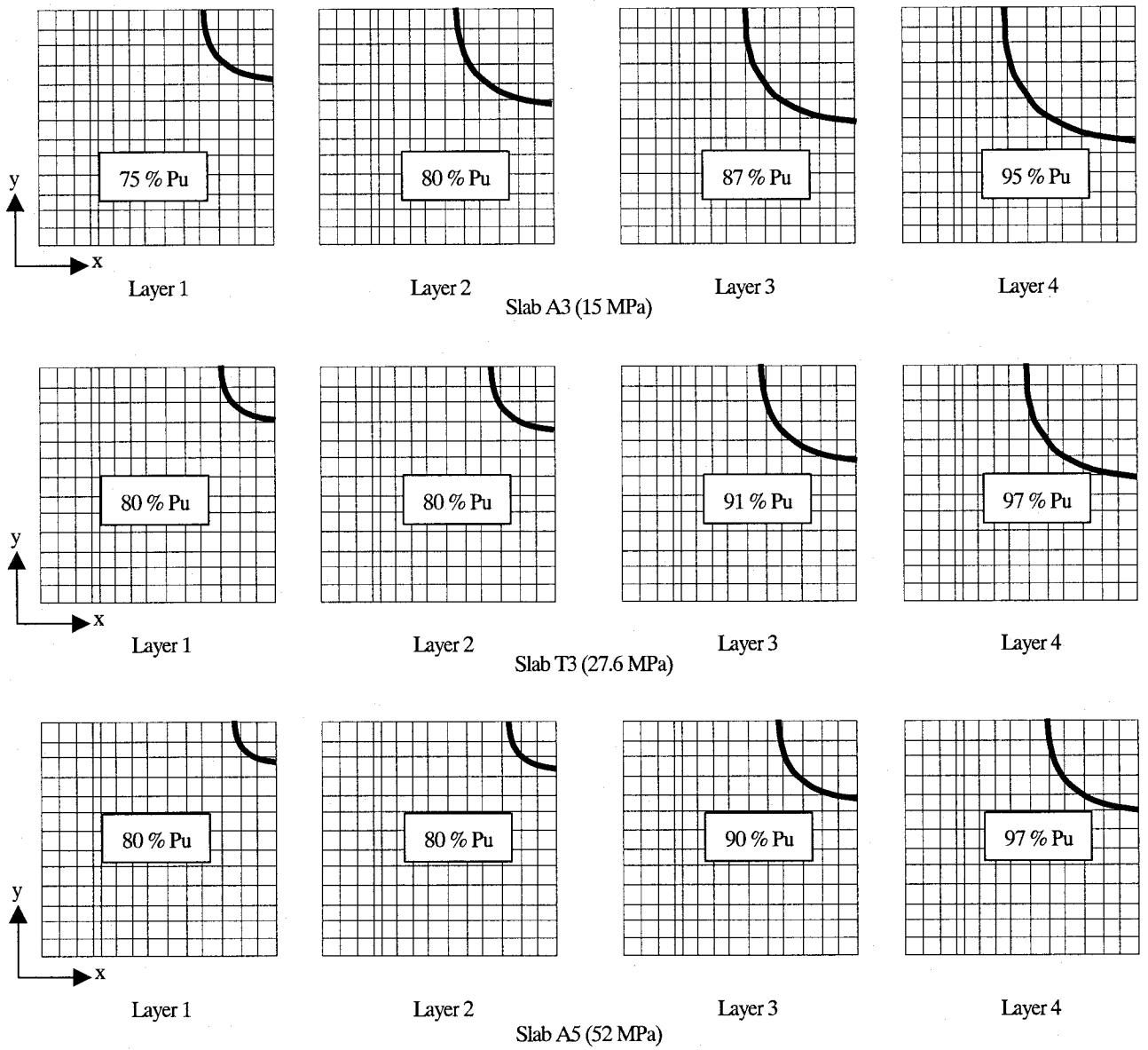

Fig. 12 Crush Path of Slabs A3, T3 and A5

In the way to find out the shape of the failure, the Gauss points at the concrete elements near the loading area had been investigated in different concrete layers, mainly in the four nearest layers to the top surface, to know the failure behavior of the punching shear of open sandwich slabs.

When the behavior of stress-strain relationship at any Gauss point is 'Unloading', the concrete is considered to be un-crushed. When 'Softening', the concrete is considered to be crushed, as shown in Fig. 13. The Gauss points had been checked out in the different layers.

In concrete layer 1 it was found a few elements had crushed and it was clear to identify the crushing front at 80 % of peak load. As the distance from the loading area increases the number of crushed elements increase, but still clear to identify the crushing front for each layer, as shown in Fig. 12.

5.3 Effect of Shear Span to Depth Ratio

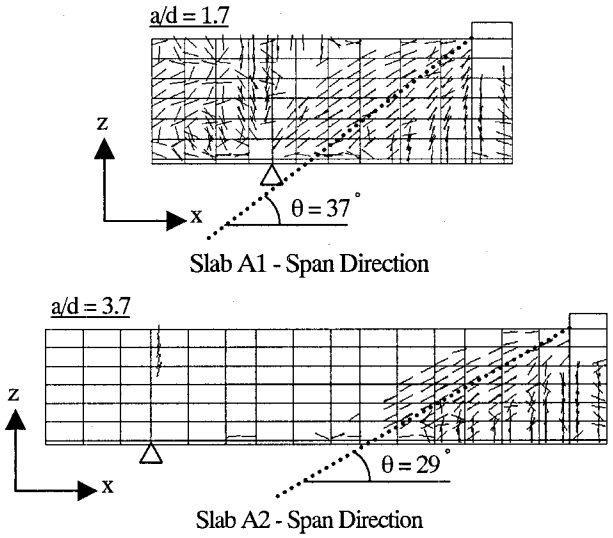

Fig. 14 Crack Pattern of Analytical Slabs at Peak Load

As we mentioned before that, it is believed that the punching shear strength decreases as shear span to depth ratio increases but in the case of the specimen slab A1 the number of studs were not enough to develop the full action of punching shear strength therefore slab A1 has failed in anchorage, meanwhile the slab A2 had a quite sufficient number of studs to develop the action of the punching shear strength. Therefore, the punching shear strength of slab A1 was less than the punching shear strength of A2.

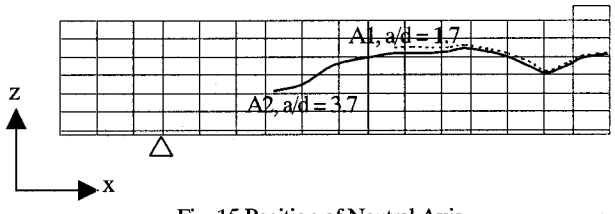

Fig. 15 Position of Neutral Axis

From Fig. 12 it is clear that the radius of the crushing front is increasing as the depth of the layer increase. Moreover, the radius is also increasing with the decreasing of the concrete compressive strength.

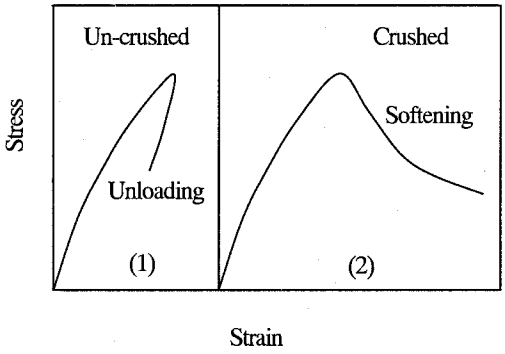

Fig. 13 Illustration of Stress-Strain Behavior

Fig. 14 shows crack pattern of the analytical slabs. It is clearly seen that the cracking angle increased as the shear span to depth ratio decreased. Moreover, it was found that the shear span to depth ratio has no effect on the depth of the neutral axis.

Fig. 15 shows that the shear span to depth ratio has no clear effect on the depth of neutral axis.

As done in the previous slabs (A3, T3 and A5) the Gauss points at the concrete elements near the top surface had been investigated to know the failure behavior of the punching shear.

In slab A1 a few elements was found to be crushed in layer 1 but more elements was found crushed in slab A2, therefore the radius of the crushing front is bigger in the case of slab A2 (Fig. 16. layer 1). Also, the main crush happens in slab A2 in earlier stage (70 % of Pu) than slab A1 (78 % of Pu). Moreover, the radius of the crushing front is increasing as the depth of the layer increases as shown in Fig. 16 – Slab A1, but in slab A2 the radius of the crushing front in layers 3 and 4 are almost the same.

It is believed that, the effect of the shear span to depth ratio is not clear and further experimental work and analytical investigation is needed.

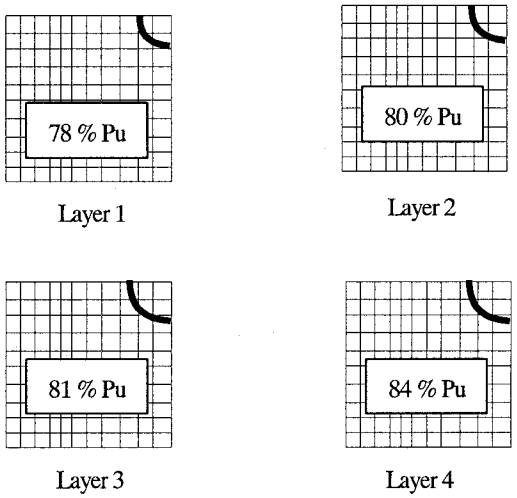

Fig. 16 (a) Slab A1 (a/d = 1.7)

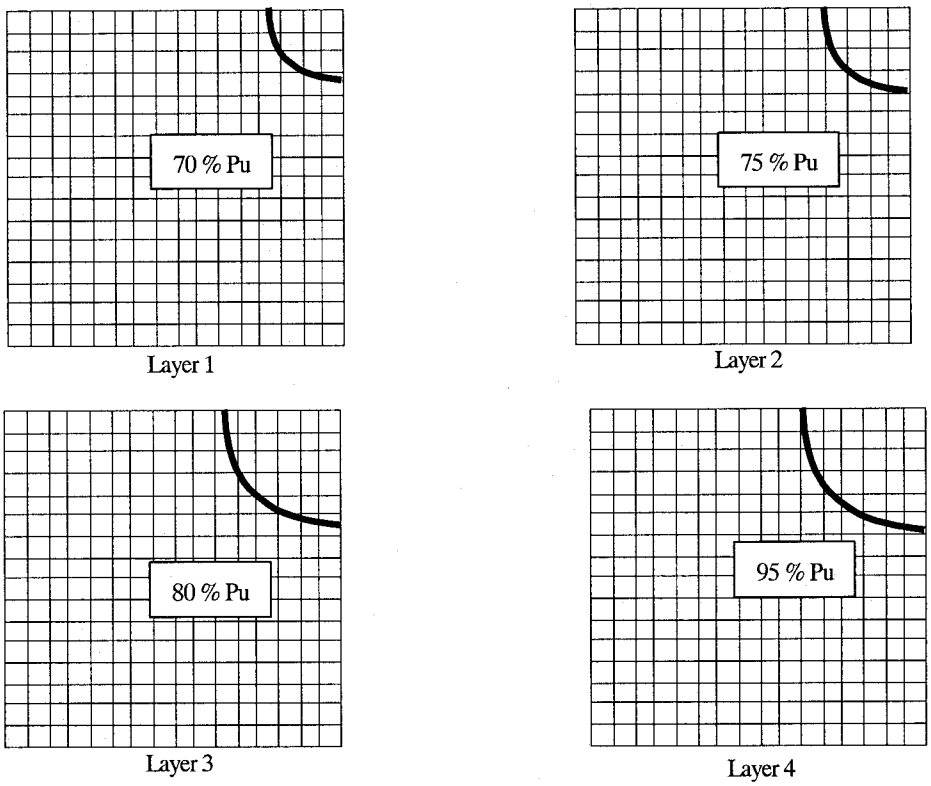

Fig. 16 (b) Slab A2 (a/d = 3.7)

Fig. 16 Crush Path of Slabs A1 and A2

5.4 Effect of Thickness of Steel Plate

The effect of the thickness of steel plate has been investigated which leads to some observations:

The depth of the neutral axis is increasing with increasing the thickness of steel plate. Actually, the thickness of steel plate is representing the percentage of the steel reinforcement in the open sandwich slab, and, as a fact, with reducing the reinforcement ratio (reduces the tensile stresses) the compression zone will be decreased (reduction of the compressive stresses) which leads to decrease the depth of the neutral axis.

However, the concrete compressive strength of slab S3 (18.5 MPa) is smaller than those of the other two specimens (26.5 MPa). Therefore, slab S3 has been re-analyzed with concrete compressive strength equal to the other two slabs (26.5 Mpa). Fig. 17 shows the load deflection curves of the re-analyzed slab S3' which used in the investigation of the effect of the thickness of the steel plate.

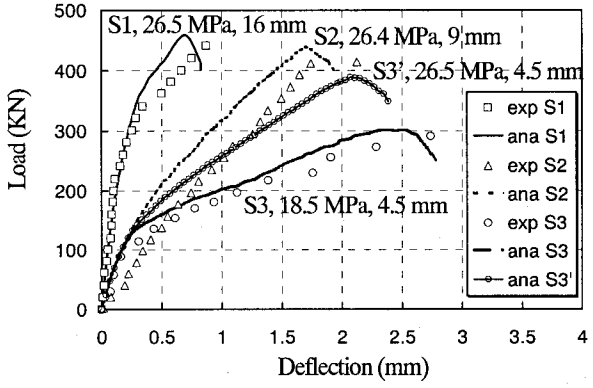

Fig 17 Load-Deflection of slabs S1, S2, S3, and S3'

The crack angles has been checked out and it was observed that no changing happen on the crack angle with different thickness of steel plate. Fig. 18 shows the crack pattern and crack angle of slab S2. It was found that the crack pattern is very similar among the three slabs (S1, S2, and S3') as well as the crack angle.

In the previous analyzed slabs the diagonal flexural cracks, which had propagated under the surface plane of neutral axis and spread toward the end sides of slab, had occurred at about 50-70 % of the ultimate load. This observation has been found on the two slabs S2 and S3' (9 mm, 4.5 mm respectively), but in the case of thick steel plate the diagonal flexural crack was observed at about 65-80 % of the ultimate load.

Moreover, as done in the previous slabs, the Gauss points at the concrete elements near the loading area had been investigated. The crushing front could be identified (Fig. 19) the radius of the crushing front is increasing with decreasing the thickness of steel plate (reduce the reinforcement ratio).

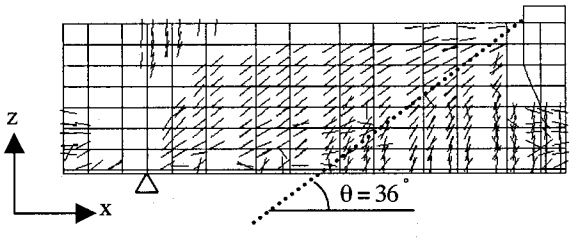

Slab S2 - Span Direction

Fig. 18 Crack Pattern of Slab S2 at Peak Load

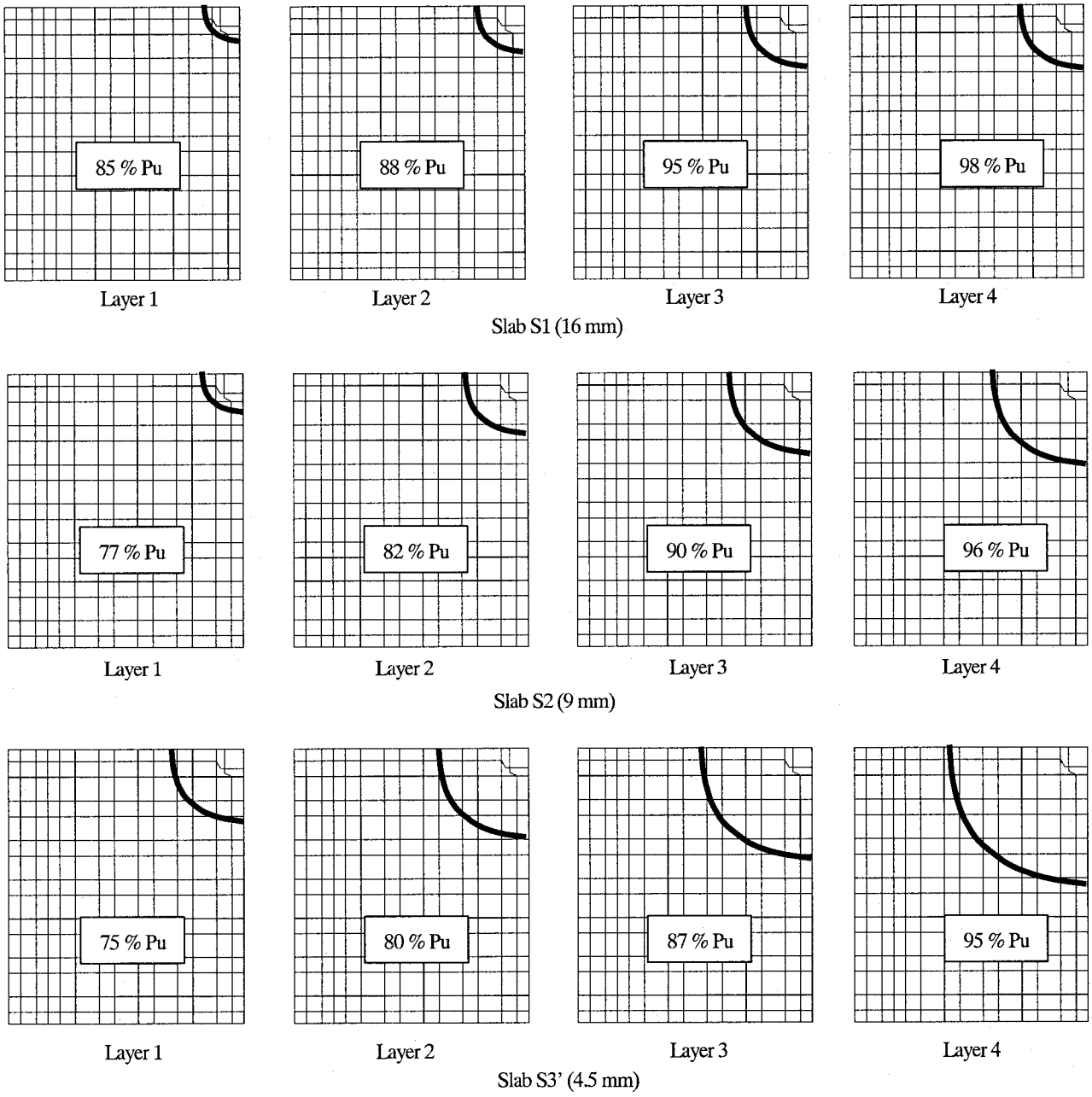

Fig. 19 Crush Path of Slabs S1, S2 and S3

5.5 Components of the Resisting Forces

Once inclined shear cracking has developed, the applied load is resisted by the vertical components of the compression zone above the crack, V_c, the aggregate interlock force, V_a, the contribution of the dowel action, V_{sp}, and the contribution of studs as shear reinforcement, V_{st}. Thus, the total shear resistance of the open sandwich slab is given by (see Fig. 20);

$$V_u = V_c + V_a + V_{sp} + V_{st} \quad (1)$$

In real behavior of punching shear mechanism of open sandwich slab these components do not remain isolated quantities, but co-exist together and, therefore, their contributions do not reach their maximum values at the same stage of loading, as experimental evidence in beams indicates [6].

It is believed that the contribution of the stud to punching shear strength is like the one of the stirrup of beam. However, there might be cases where stud heads are not well anchored. Therefore, the local stresses around the stud head might affect the punching shear strength. Thus, this point will be taken into consideration on developing the punching shear strength formula.

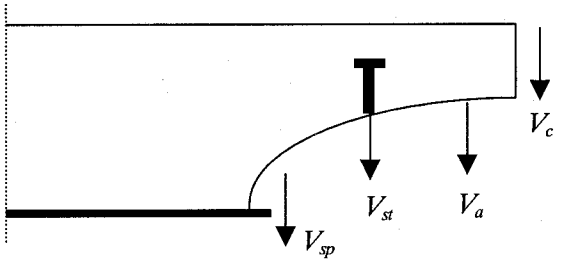

Fig.20 Illustration of Resisting Force Components

The portion of the load resisted by the compression zone is dependant upon the area of slab above the inclined crack, and the shear resistance of concrete. The aggregate interlocking effect, which activates only after the appearance of inclined cracking, depends on concrete properties, crack width and the relative displacement between the two faces of crack due to the rotation about the head of the crack [9]. However, the aggregate interlocking force is activated only after the formation of the inclined crack. The dowel action has a small contribution, as its value is less than 2% of the punching shear strength. The dowel force has been calculated at three different positions as shown in Table 3.

Table 3. Dowel Force

Slab	Ultimate Load (KN)	Dowel Force (KN)			Percentage %		
		P1	P2	P3	P1	P2	P3
A1	417.0	4.51	7.94	6.01	1.08	1.90	1.44
A2	477.1	4.89	7.49	6.75	1.02	1.57	1.41
A3	249.2	2.52	4.86	3.72	1.01	1.95	1.49
T3	395.4	5.49	7.32	6.80	1.39	1.85	1.72
A5	564.2	6.09	8.81	7.29	1.08	1.56	1.29

Neglecting the dowel action , Eq. (1) can be written as

$$V_u = V_c + V_a + V_{st} \quad (2)$$

The vertical component of the compression zone above the crack is a function of the concrete compressive strength, shear span to depth ration and thickness of steel plate

6. Conclusion

The present study was conducted on analytical simulation of a series of tests of open sandwich slabs. The aim was to study the effect of concrete compressive strength, shear span to depth ratio, and thickness of steel plate on the punching shear strength of the open sandwich slabs. From the analysis of the experimental results we can conclude the effect of the parameters as follow; the punching shear capacity increases with the increase of concrete compressive strength, the effect of shear span to depth ratio could not seen clearly probably due to experimental scatter, further experimental study is necessary, and the punching shear strength is increasing as the thickness of steel plate is increasing.

The punching failure of the open sandwich slabs was successfully simulated with this numerical model. The mode of failure (characterized by a localized inclined crack) and the sequence of cracking were reproduced. Non-linear finite element analysis can predict the ultimate load and deformational behavior with reasonable accuracy.

The finite element analysis indicates that the way of meshing has an effect on the analytical result and that the discrete way of analysis is more reliable than the smeared way.

The concrete compressive strength and the thickness of steel plate have a clear effect on the position of the neutral axis that can differentiate between the two kinds of the cracks occurs in the slabs (circular cracks, and diagonal flexural cracks). Therefore, it could be one of the keys to come up with the prediction formula for punching shear strength of open sandwich slabs.

Punching shear failure occurs in the compression zone due to crushing of the concrete near the top surface. Moreover, it was observed that, the concrete layers near the top surface of the slab crushed earlier than the concrete layer far from the top surface.

The crushing front at each layer of the analyzed slabs could be identified and was noticed that, the radius of the crushing front is increasing as the depth of the investigated layer increased. Furthermore, the radius of the crushing front is increasing with the decreasing of the concrete compressive strength and decreasing the thickness of steel plate.

The dowel force has a slight contribution to the punching shear strength while the vertical component of the compression above the cracks and the contribution of the stud as shear reinforcement have a pronounced effect and characterized by increase its value by increase of the concrete compressive strength and the thickness of steel plate. Moreover, the contribution of the aggregate interlocking needs further investigation to clarify its effect.

Depending on the results of the shown study a quantitative study will be done to identify the contribution of each components of the resisting forces numerically. Based on the quantitative study an expression to calculate the punching shear strength will be developed in future study.

References

1) Takahashi, R., Analysis of Concrete Member Behavior by Three-dimensional Non-linear Finite Element Analysis, Doctor Dissertation, Hokkaido University, 2003

2) Maekawa, K. et. al., Triaxial Elasto-Plastic and Fracture Model for Concrete, Proceeding of JSCE, Vol.18, No.460, pp.131-138, 1993.

3) Takahashi, R., Ueda, T. and Sato, Y., Study on Punching Shear Failure of Steel-Concrete Sandwich Slab, Proc. of the ICCMC/IBST 2001, International Conference on Advanced Technologies in Design, Construction and Maintenance of Concrete Structures, Hanoi, Vietnam, pp.182-187, 2001.

4) Farghaly, A., Ueda, T., Konno, K. and Takahashi, R., 3D FEM Analysis of Open Sandwich Beams, Proceeding of the Japan Concrete Institute, Vol. 24, No. 2, pp. 103-108, 2002.

5) Standard Specification of Design and Construction of Concrete Structures, JSCE, 1991.

6) Swamy, R. and Andriopoulos, A., Contribution of Aggregate Interlock and Dowel Forces to the Shear Resistance of R.C. Beams with Web Reinforcement, ACI Publication, SP-42, 1974.

(Received September 12, 2003)